Scanning Microscopy

Volume 6 | Number 4 Article 10

9-29-1992

Scanning Electron Microscopy Observation of the Interaction Between the Surface Acoustic Waves and Regular Domain Structures in the LiNbO3 Crystals

D. V. Roshchupkin
Laboratoire de Cristallographie

Th. Fournier
Laboratoire de Cristallographie

M. Brunel
Laboratoire de Cristallographie

O. A. Plotitsyna
Laboratoire de Cristallographie

N. G. Sorokin
Moscow Institute of Steel and Alloys

Scanning Microscopy, Vol. 6, No. 4, 1992 (Pages 993-996) 0891-7035/92$5.00+.00
Scanning Microscopy International, Chicago (AMF O'Hare), IL 60666 USA

SCANNING ELECTRON MICROSCOPY OBSERVATION OF THE INTERACTION BETWEEN THE SURFACE ACOUSTIC WAVES AND REGULAR DOMAIN STRUCTURES IN THE $LiNbO_3$ CRYSTALS

D.V. Roshchupkin[1,2,*], Th. Fournier[1], M. Brunel[1], O.A. Plotitsyna[1,2] and N.G. Sorokin[3]

[1]CNRS, Laboratoire de Cristallographie, 166X - F-38042 Grenoble cedex, France
[2]Institute of Problems of Microelectronics Technology and Superpure Materials, Russian Academy of Sciences, 142432 Chernogolovka, Moscow District, Russia
[3]Moscow Institute of Steel and Alloys, Moscow, Russia

(Received for publication April 17, 1992, and in revised form September 29, 1992)

Abstract

This paper reports a scanning electron microscope study of the interaction between the surface acoustic waves and regular domain structures in $LiNbO_3$ crystals. The regular domain structures in $LiNbO_3$ crystals were formed by the method of the thermo-electric treatment after growth. We investigated two modes of interaction: the surface-acoustic-waves propagate along and across the regular domain structures. It is shown that the regular domain structures in the first case can be used as an acoustical wave-guide, because the power-flow vector of the surface acoustic waves has the direction along the domain structure. Also we observed that the surface acoustic wave inverts the voltage contrast of the image in the scanning electron microscope by π during the process of the propagation across the domain walls.

Key Words: Surface acoustic waves, voltage contrast, regular domain structure.

*Address for correspondence:
Dmitry Roshchupkin
CNRS Laboratoire de Cristallographie
166X
F-38042 Grenoble cedex FRANCE
Telephone Number: (33) 76 88 10 46
FAX Number: (33) 76 8810 38

Introduction

Today, the scanning electron microscopy (SEM) is one of the best methods for the observation of surface and bulk acoustic wave propagation in piezoelectric materials [2-5, 8, 9, 11]. The SEM in the secondary electron emission mode permits to visualize the electric potential distribution on the crystal surface, as the low energy secondary electrons (1-3 eV) are sensitive enough to the electric field, which accompanies the propagation of the traveling surface acoustic waves (SAW) in the piezoelectric materials. We have investigated the interaction between the SAW and regular domain structures in the $LiNbO_3$ crystals.

Experimental Details

These experiments have been performed at Centre National de la Recherche Scientifique, Grenoble, using a JEOL JSM-840 SEM. We have used the autostroboscopic mode of the SEM described in a number of papers [6, 7]. In this mode of the SEM, the image of the SAW is formed by high-frequency modulation of the low energy secondary electrons. This results in a stationary electrostatic interference field formed above the crystal surface due to the interaction between the varying electrostatic field of the SAW and the component (normal to the surface) of the electromagnetic radiation field of the interdigital transducer (IDT). The electromagnetic and acoustic waves are mutually coherent, since they are excited by the same source (IDT) and with the same frequency. The difference in phase between electromagnetic and electrostatic waves is given by:

$$\phi = 2\pi L\ [(1/\Lambda_{SAW}) - (1/\lambda_e)] = (2\pi L/\lambda_e)\ (n_a^*-1),$$

where Λ_{SAW} is the SAW wavelength, λ_e the wavelength of electromagnetic radiation, n_a^* the effective refractive index for the electrostatic wave propagating along the crystal surface, and L the distance from the interdigital transducer. If we assume that the velocity of the electromagnetic wave in vacuum is the speed of light (c) and that the velocity of a sound wave in the $LiNbO_3$ crystal is ~ 3500 m/s, then we obtain the effective refractive index for the electrostatic wave: $n_a^* \approx 8.6 \cdot 10^6$, i.e., $n_a^* >> 1$. This means that a stationary interference field with a wavelength Λ_i is formed above the surface of the crystal and with a relative accuracy of ~ 10^{-7}, the wavelength coincides with Λ_{SAW}; this condition was observed experimentally. However, according to the general theory of coherence, the interference pattern may be observed only in matter; the interaction process is described by the matrix element for the transition of atoms into new states, and there is no photon-photon interaction. In this case, the recording medium is a cloud of secondary electrons which have left the surface through the action of the primary electron beam. Evidently there is also an interference polarization of the crystal surface, with a period close to that of the acoustic wave (since $\Lambda_i \approx \Lambda_{SAW}$).

Experimental Results and Discussion

For our investigations we used two types of substrates with regular domain structures: ZX-cut and YX-cut of the $LiNbO_3$ crystals. Regular domain structures with domain width ~ 60 μm were formed in ferroelectric substrates by the method of thermo-electric treatment after growth near the Curie temperature (T_C ~ 1100 °C) at the conditions for the temperature gradient and electric field [1]. The neighbouring domains distinguish by the opposite directions of the polar axis Z and piezoelectric axis Y (plus or minus), respectively.

Fig. 1 demonstrates the experimental scheme, when the SAW propagates in ZX-cut of the $LiNbO_3$ crystal along the domain structure in the direction of the axis X. For excitation of the SAW an IDT with a 15 μm period and 30 μm SAW wavelength was formed on the surface of the ZX-cut of the $LiNbO_3$ crystal so that the SAW propagates with propagation vector along the direction of the axis X. The SAW velocity along axis X is V = 3.7976 km/s. The regular domain structure in this substrate was formed in such a manner that the angle between the domain walls and direction of the axis X was ~ 10°.

Fig. 2 shows the SEM photomicrographs of the propagation of the traveling SAW. The SAW pattern was visible at an accelerating voltage E_o = 1-2 kV and a probe current $I_o = 6 \cdot 10^{-9}$ A. The use of higher accelerating voltage (> 3 kV) was not possible, because the insulating substrate became highly charged and led to a distortion of the image due to deflection of electrons [10]. Fig. 2a shows the SEM micrograph of radiation pattern of an interdigital transducer excited at the resonance frequency f_o = 126.59 MHz. This value of the resonance frequency is in a good agreement with the one calculated from the classical formula $V = \Lambda_{SAW} \cdot f$ (V = 3.7976 km/s, Λ_{SAW} = 30 μm). The amplitude of the input signal U on the IDT was 10 V. It is seen from the contrast of the SEM image that the energy of the SAW propagates along the domain structure (more brightness contrast, which corresponds to the largest amplitude of the SAW). The propagation of the energy of the SAW is characterized by the power-flow vector (PFV) with the direction along the domain structure. Fig. 2a shows that the power-flow angle ϕ equals 10°,

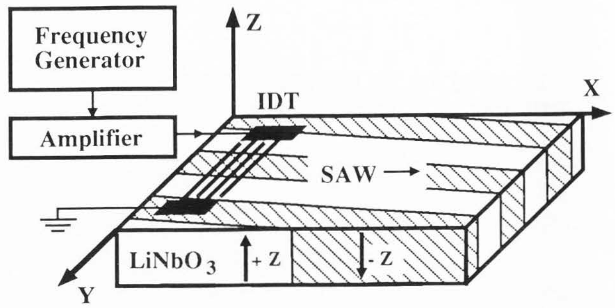

Figure 1 (above). Experimental scheme showing the SAW propagation in the ZX-cut of the $LiNbO_3$ crystal along axis X.

Figure 2 (facing page, left). SEM photomicrographs of the propagation of the traveling SAW: (**a**) radiation pattern of an IDT excited out of band at f_o = 126.59 MHz (IDT - interdigital transducer, PFV - power-flow vector); (**b**) inversion of the voltage contrast image of the SAW by π on the domain wall AB; and (c) defect of irregularity in the regular domain structure.

i.e., the angle between the direction of the power-flow vector and the direction of the propagation vector. This angle is equal to the angle between the domain walls and direction of the axis X. It means that in this case the regular domain structure acts as an acoustic wave-guide. Fig. 2b demonstrates the propagation of the traveling SAW along the regular domain structure at high magnification (X200). It is seen that the traveling SAW inverts the voltage contrast of the image by π on the domain wall AB, because the neighbouring domains in this case are antiparallel to the polar axis Z, and maxima of the surface acoustic waves in one domain have the opposite potential than in the neighbouring domain. The positive potential decreases the number of detected secondary electrons from the crystal surface and has dark contrast, while negative potential increases the number of detected secondary electrons and has bright contrast. The inversion of the potential changes the coefficient of the secondary electron emission and, by this, inverts the voltage contrast of the image of the SAW by π. Also, it has been seen that the angular divergence of the acoustic beam, which propagates along the regular domain structure, is practically absent. Fig. 2a also demonstrates that it is very difficult to observe an image of the regular domain structure on the crystal surface without SAW. With high magnification also, it was not possible to observe the regular domain structure. In this case, it was necessary to excite the SAW for observation of the domain structure in the ferroelectric crystals. Fig. 2c shows the image of the surface defect in the regular domain structure, which was observed only by exciting the SAW on the crystal surface. We visualized the tear in the domain wall CD and formation of two new domain walls CF and DE. This defect was formed at the process of the regular domain structure formation.

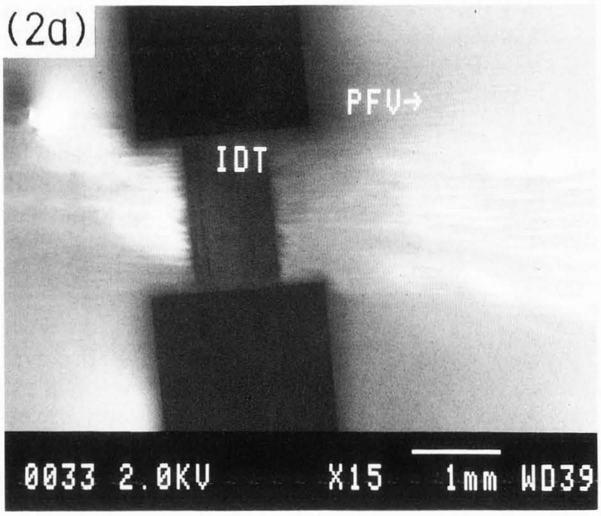

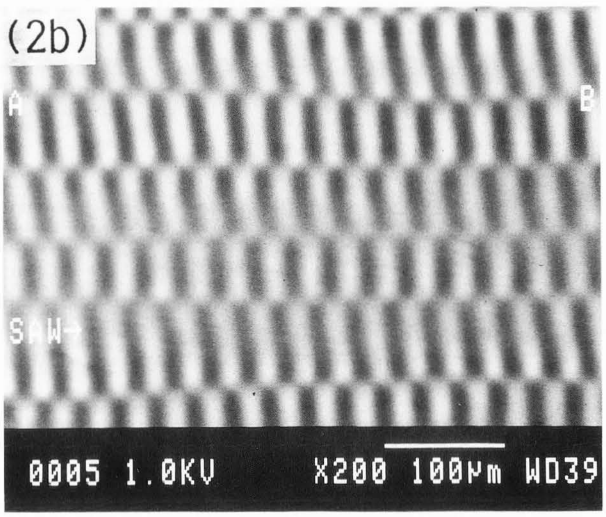

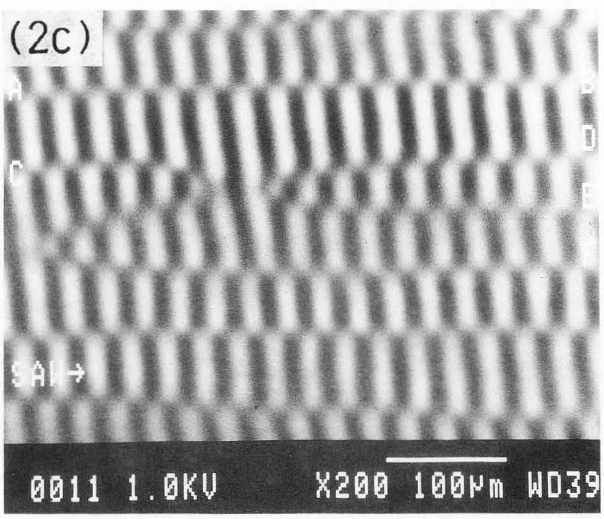

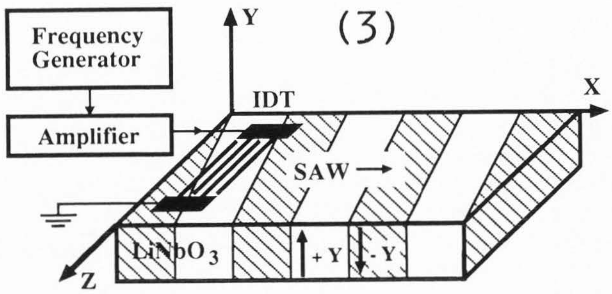

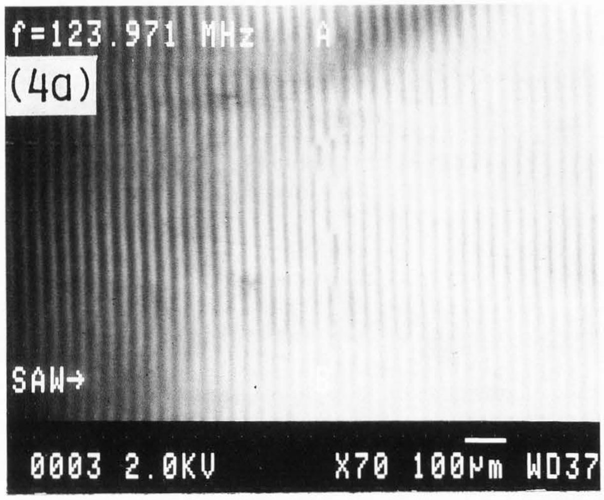

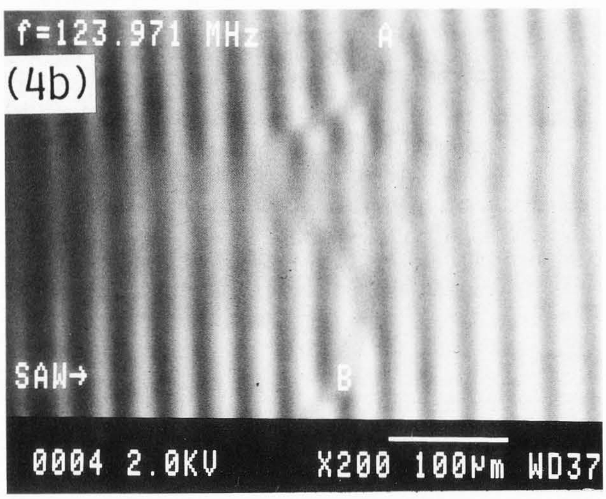

Figure 3 (top). Experimental scheme showing the SAW propagation across the regular domain structure in the YX-cut of the $LiNbO_3$ crystal along axis X.

Figure 4a,b (bottom). SEM photomicrographs of the propagation of the traveling SAW: (**a**) inversion of the voltage contrast of the image of the SAW by π on the domain wall AB in YX-cut of the $LiNbO_3$ crystal; (**b**) roughness of the domain wall AB.

Fig. 3 shows the experimental arrangement when the SAW propagates across a regular domain structure. An IDT with the SAW wavelength 30 μm and resonance frequency f_0 = 123.97 MHz, respectively, was formed on the YX-cut of the $LiNbO_3$ crystal. The SAW propagates along X-axis across the domain structure with velocity V = 3.7690 km/s. The SAW inverts the voltage contrast of the image by π on the domain wall AB (Fig. 4), because the neighbouring domains in this cut have the opposite directions of the piezoelectric axis Y. It means that the maximums of the SAW have the opposite potentials in the neighbouring domains and are distinguished by the number of detected secondary electrons. At high magnification (X200), Fig. 4b demonstrates the roughness of the domain wall AB.

Conclusions

This paper demonstrates, for the first time, the interaction between the traveling surface acoustic waves and regular domain structures. We have shown the possibility to use the regular domain structures as an acoustic wave-guide, because the energy of the SAW propagates along the domain structure. Also, we demonstrated that the SAW inverts the voltage contrast of the image by π on the domain walls with the propagation of SAW. This makes it possible to use SAW for observation of the domain structure in the ferroelectric crystals.

References

1. Antipov VV, Blistanov AA, Sorokin NG, Chizhikov SI (1985) Formation of regular domain structure in the ferroelectrics $LiNbO_3$ and $LiTaO_3$ near the phase transition. Sov. Phys. Crystallogr. **30**, 428-430.

2. Bahadur H, Parshad R (1980) Scanning electron microscopy of vibrating quartz crystals. Scanning Electron Microscopy **1980**; I: 509-522.

3. Bahadur H, Hepworth A, Lall VK, Parshad R (1978) Electron contrast effects from oscillating quartz crystals seen by the scanning electron microscope. IEEE Trans. Sonics and Ultrasonics **SU-25**, 309-313.

4. Bahadur H, Parshad R, (1980) Scanning electron microscopy of vibrating quartz crystals - a survey. IEEE Trans. Sonics and Ultrasonics **SU-27**, 303-317.

5. Bahadur H, Parshad R (1985) SEM observations of mode shapes of flexural, anharmonic, and thickness-shear vibrations in quartz resonators. IEEE Trans. Sonics and Ultrasonics **SU-32**, 861-864.

6. Bert AG, Epsztein B, Kantorowicz G (1972) Charge storage of acoustic rf signals. Appl. Phys. Lett. **21**, 50-52.

7. Dremova NN, Erko AI, Roshchupkin DV (1988) Charging mechanism for the formation of a metastable surface-acoustic-wave potential contrast observed in a scanning electron microscope. Sov. Phys. -Tech. Phys. **33**, 1066-1068.

8. Eberharter G, Feuerbaum HP (1980) Scanning-electron-microscope observations of propagating acoustic waves in surface acoustic wave devices. Appl. Phys. Lett. **37**, 698-699.

9. Feuerbaum HP, Eberharter G, Tobolka G, (1980) Visualization of traveling surface acoustic waves using a scanning electron microscope. Scanning Electron Microscopy **1980**; I: 503-508 and 502.

10. Goldstein JI, Yakowitz H (eds.) (1975) Practical Scanning Electron Microscopy: Electron and Ion Microprobe Analysis. Plenum Press, 212-216, 253-254.

11. Tanski WI, Wittels ND (1979) SEM observations of SAW resonator transverse modes. Appl. Phys. Lett. **34**, 537-539.

Discussion with Reviewers

H. Bahadur: Did you attempt to obtain the time-averaged micrographs? If so, is there any difference in patterns between time-averaged micrographs and those obtained using the stroboscopic technique?
Authors: In our investigations, we did not observe any difference in patterns between the time-averaged micrographs and those obtained using the stroboscopic technique. Also, by the time-averaged technique it is possible to observe the SAW pulses such as it was observed using the stroboscopic technique in ref.9.

H. Bahadur: Have you noticed any bulk wave pattern in addition to the SAW? Perhaps, an useful information could be obtained if the piezoelectric resonator is excited to the bulk oscillating frequency using IDT.
Authors: No, in this experiment we did not observe any bulk wave pattern.

H. Bahadur: Sometimes very complex patterns are observed in such investigations. I imagine you also must have come across such cases. Was it possible for you to clearly attribute these patterns to any other form of the traveling waves such as Rayleigh, Love, Lamb or Stoneley waves?
Authors: Here, we investigated the propagation of the Rayleigh waves. But using the time-averaged technique we can differentiate forms of traveling waves.

H. Bahadur: Have you measured the vibrational amplitude using the technique described in the paper? If so, what is the order of the magnitude? Is there any evidence of the change of the direction of vibrations on the resonator surface?
Authors: We did not measure the vibrational amplitude using this technique. In this case there is no other evidence of the change of the power-flow vector direction.

L. Balk: The contrast of the secondary electron image is mainly due to potential variation at the surface, as you state. Is the method applicable only when the domain appears at the surface? Is there an effect if there is a modification of the surface (by ions for example)?
Authors: This method is applicable for all types of investigation of the SAW propagation. The modification of the surface (by ions) can change the sound velocity on the crystal surface and it is possible to observe this effect by SEM, but really it would depend on the extent of surface modification which again would be a function of energy, dose and area of cross-section of the impinging ions on the sample.